Monte Carlo and Mean Field Study of Diblock Copolymer Micelles

M. P. Pépin† and M. D. Whitmore*

Department of Physics and Physical Oceanography, Memorial University of Newfoundland, St. John's, Newfoundland, Canada, A1B 3X7

Received December 21, 1999; Revised Manuscript Received August 9, 2000

ABSTRACT: When small concentrations of A-*b*-B diblock copolymer are mixed with selective solvent or A homopolymer, they often form spherical micelles with cores comprised of the B blocks. Mean field theory predicts that the core radii scale primarily with the degree of polymerization of the B block as Z_{CB}^{α} with $\alpha \simeq 2/3$ or larger, and this is consistent with many experimental data. However, recent experiments on very strongly segregated "crew-cut" micelles indicate a much weaker dependence. In this paper, we study crew-cut micelles using a simple mean field theory and Monte Carlo simulations. The Monte Carlo simulations include the calculation of the system relaxation times, which are used both to determine the simulation times required to reach equilibrium and to examine, at least qualitatively, the variable solvent qualities at which the micelle structures become "frozen in" for different polymer molecular weights. The mean field results for these crew-cut, strongly segregated micelles are consistent with previous mean field calculations, giving $\alpha = 0.77$ at fixed solvent quality. The Monte Carlo results indicate that nonequilibrium effects result in a weaker power law, as observed experimentally.

1. Introduction

Block copolymers are used in a wide variety of applications. The addition of small amounts of A-*b*-B diblock copolymers to a selective solvent can result in the formation of micelles which, if the overall copolymer concentration is low enough, are randomly distributed throughout the host. The incompatible copolymer block, which we take to be the B block here, forms the core of the micelles, and the A block forms a corona. There has been considerable theoretical and experimental interest in the study of micelles where the B block of the copolymer is short compared to the A block, resulting in a relatively small core compared to the corona. Recently, there has been interest in the experimental study[1,2] of so-called "crew-cut" micelles where the B block is larger than the A block. These micelles have relatively large cores compared to the thickness of the corona.

Of particular interest in all these systems is the radius of the micelle core, l_B, and the thickness of the corona, l_A, as functions of the degrees of polymerization of the A and B blocks, Z_{CA} and Z_{CB}, respectively. de Gennes[3] predicted a scaling relation for the core radius, $l_B \propto Z_{CB}^{\alpha}$, with $\alpha = 2/3$. Leibler et al.[4] extended this work by minimizing the total free energy of the system, allowing a fraction of copolymers to remain free in solution. For fixed copolymer composition (fixed Z_{CB}/Z_{CA}), the core radius again scaled as Z_{CB}^{α} with $\alpha = 2/3$. Noolandi and Hong[5] performed mean field calculations on diblock copolymer micelles in selective solvent with fixed Z_{CB}/Z_{CA} and obtained $l_B \propto Z_{CB}^{\alpha}$ with $\alpha = 0.64$. The radius of the entire micelle, $l = l_B + l_A$, was found to scale as $l \propto Z_C^{\gamma}$ with $\gamma = 0.68$. Whitmore and Noolandi[6] extended this work, varying Z_{CA} and Z_{CB} independently. They found

$$l_B \propto Z_{CB}^{\alpha} Z_{CA}^{\beta} \tag{1}$$

with $0.67 \leq \alpha \leq 0.76$ and $-0.1 \leq \beta \leq 0$. For the corona thickness, they found $l_A \propto Z_{CA}^{\nu}$ with $0.5 \leq \nu \leq 0.86$. Nagarajan and Ganesh[7] performed a similar calculation but with polydisperse systems of micelles. They obtained similar results for l_B with $0.70 \leq \alpha \leq 0.73$ and $-0.17 \leq \beta \leq -0.08$, and $l_A \propto Z_{CB}^{\mu} Z_{CA}^{\nu}$ with $0.06 \leq \mu \leq 0.07$ and $0.68 \leq \nu \leq 0.74$.

All these theories assumed a constant volume fraction profile for each constituent in the micelle core and corona. Halperin[8] noted that micelles are structurally similar to colloidal particles coated by grafted chains, and to star polymers. Therefore, he performed a scaling analysis of the micelle structure by adapting the theory of Daoud and Cotton[9] for star polymers. He considered the two limiting cases of $Z_{CA} \gg Z_{CB}$ and $Z_{CA} \ll Z_{CB}$. The first case, which corresponds to relatively short core blocks, gives $l_B \propto Z_{CB}^{\alpha}$ with $\alpha = 3/5$ and $l \propto Z_{CB}^{\alpha} Z_{CA}^{\beta}$ with $\alpha = 4/25$ and $\beta = 3/5$. The second case corresponds to crew-cut micelles, and $l \approx l_B \propto Z_{CB}^{\alpha}$ where $\alpha = 2/3$.

There have been a number of more sophisticated theoretical treatments of self-assembly and micelle formation in these and similar systems. They include lattice-based numerical self-consistent field (NSCF) calculations of the volume fraction profiles,[10−13] single chain mean field calculations[14,15] (SCMF), molecular dynamics[16] (MD), and Monte Carlo[13,17−26] (MC) simulations. In particular, Mattice et al.[17−26] have done extensive MC studies of diblock copolymer micelles. None of these approaches have been used to investigate scaling relations.

Experiments on the structure of polystyrene-*b*-poly(ethylene oxide) (PS-*b*-PEO) block copolymer micelles in cyclopentane and deuterated cyclohexane were done by Gast et al.[27] They concluded that the starlike model was best suited for describing density profiles in micelles with moderate aggregation numbers and long corona blocks. Selb et al.[28] did small-angle neutron scattering (SANS) experiments on poly(styrene-*b*-butadiene) diblock copolymers in polybutadiene. The experimental results showed micelles with a narrow size distribution. Whitmore and Noolandi[6] did a scaling analysis of these

† Current address: Department of Physics, University of Ottawa, 150 Louis-Pasteur, Ottawa, ON, Canada, K1N 6N5.

10.1021/ma992135z CCC: $19.00
Published on Web 10/21/2000

Table 1. Theoretical and Experimental Scaling Laws[a]

	$l_B \propto Z_{CB}^{\alpha} Z_{CA}^{\beta}$		$l_A \propto Z_{CB}^{\mu} Z_{CA}^{\nu}$	
authors	α	β	μ	ν
de Gennes[3,b]	2/3			
Leibler et al.[4,b]	2/3			
Hong et al.[5,b]	0.64			
Whitmore et al.[6,b]	0.67−0.76	−(0−0.1)	0	0.5−0.86
Nagarajan et al.[7,b]	0.70−0.73	−(0.08−0.17)	0.06−0.07	0.68−0.74
Halperin[8] $Z_{CB} \ll Z_{CA}$[b]	3/5			
Halperin[8] $Z_{CB} \gg Z_{CA}$[b]	2/3			
Selb et al.[28,c]	0.75−0.81	−(0.14−0.19)		
Bluhm et al.[32,b]	0.67	−0.17	0.12	0.54
Zhang et al.[1,c]	0.4	−0.15		
mean field theory (current)[b]	0.77	−0.18	−0.051	0.864

authors	
Hong et al.[6,b]	$l \propto Z_C^{\gamma}$, $\gamma = 0.68$
Halperin[8] $Z_{CB} \ll Z_{CA}$[b]	$l \propto Z_{CB}^{\alpha} Z_{CA}^{\beta}$, $\alpha = 4/25$ and $\beta = 3/5$
Halperin[8] $Z_{CB} \gg Z_{CA}$[b]	$l \approx l_B \propto Z_{CB}^{\alpha}$, $\alpha = 2/3$
Munk et al.[31,b]	$R_H \propto Z_{CB}^{\alpha} Z_{CA}^{\beta}$, $\alpha = 0.71$ and $\beta = -0.09$
Hurtrez[33,b]	$R_H \propto Z_C^{\gamma}$, $\gamma = 0.36$
Hurtrez[33,c]	$R_H \propto Z_{CB}^{\alpha} Z_{CA}^{\beta}$, $\alpha = 0.09$, $\beta = 0.31$
Hurtrez[33,c]	$R_H = 1.01 Z_{CB}^{\alpha} Z_{CA}^{\beta} + 0.78 Z_{CB}^{\mu} Z_{CA}^{\nu}$ $\alpha = 0.75$, $\beta = -0.17$, $\mu = -0.53$, $\nu = 0.74$
Bluhm et al.[32,b]	$R_M \propto Z_C^{\gamma}$, $\gamma = 0.44$

[a] l_B is the core radius, l_A is the thickness of the corona, $l = l_B + l_A$, R_H is the hydrodynamic radius, and R_M is the radius of gyration of the micelle. [b] Theoretical. [c] Experimental.

experimental results. The micelle core radii scaled according to eq 1, with $0.75 \leq \alpha \leq 0.81$ and $-0.19 \leq \beta \leq -0.14$. In the same study, Whitmore and Noolandi[6] also made a direct comparison of these experiments with their simple mean field theory, which assumed a single size distribution of micelles. The scaling exponents for the core radii were consistent with those from the experiments, as shown in Table 1. Liu et al.[29] performed experiments on polystyrene-*b*-poly(2-cinnamoylethyl methacrylate) block copolymer micelles in cycloheptane. They observed that the core radius could be well represented by the scaling laws predicted from existing theories. Similar results were obtained by Kinning et al.[30] for poly(styrene−butadiene) block copolymer micelles in a polystyrene homopolymer. Munk et al.[31] found that the measured hydrodynamic radius of polystyrene-*b*-poly(methacrylic acid) block copolymer micelles in dioxane and water scaled according to eq 1, with $\alpha = 0.71$ and $\beta = -0.09$. In all these cases, $l_B \propto Z_{CB}^{\alpha}$ with $\alpha \geq 0.6$, in general agreement with theory.

There are, however, other experiments that give different scaling relations. Bluhm and Whitmore[32] measured the radius of gyration of PS-*b*-PBD micelles in heptane, R_M, and found an effective scaling of $R_M \propto Z_C^{\gamma}$ with $\gamma = 0.44$. This was fully explained by mean field theory, as due to the variable chemical composition of the molecules used in the experiments, i.e., different relative block lengths. More recently, Hurtrez[33] performed experiments on PS-*b*-PEO copolymers in water with short PS blocks and long PEO blocks forming the core and corona of the micelles, respectively. The author measured the hydrodynamic radius R_H of the micelles and fitted powers to the scaling functions predicted by the theories of Hong and Noolandi, Halperin, and Nagarajan and Ganesh, and found $R_H \propto Z_C^{0.36}$, $R_H \propto Z_{CB}^{0.09} Z_{CA}^{0.31}$ and $R_H = 1.01 Z_{CB}^{0.75} Z_{CA}^{-0.17} + 0.78 Z_{CB}^{-0.53} Z_{CA}^{0.74}$, respectively. The comparison between experimental and theoretical results can be seen in Table 1. The important point is that the first two scaling laws show weak dependences on the degrees of polymerization. However, it should be noted that the measured micelle radii were very small, in some cases comparable with the radii of gyration of a single molecule. Zhang et al.[1] studied crew-cut micelles composed of polystyrene-*b*-poly(acrylic acid) block copolymers in water. They measured the core radii by transmission electron microscopy and found them to scale according to eq 1 with $\alpha = 0.4$ and $\beta = -0.15$. Again, the point to be noticed is the weak dependence of the radii on the core block. The authors noted that this may be due to nonequilibrium effects; if so, similar effects might apply to the systems studied by Hurtrez.

These observed weak dependences on Z_{CB} and the ability of simple mean field theory to explain some of them implies that further theoretical studies of micelles, and in particular crew-cut micelles, are warranted. In the work reported here, we study crew-cut micelles using both MC simulations and simple mean field theory. The mean field calculations are done to see if the weak scaling of the crew-cut micelles can be explained as an equilibrium effect, as was the case for the PS-*b*-PBD micelles. Although the model used is much simpler than, for example, NSCF theories, it is well suited for the systematic calculations needed to obtain scaling laws, and has worked well on noncrew cut micelles. The MC simulations are performed to probe the assumptions made in the mean field approach regarding the structure and size distributions of the micelles, to complement the mean field studies by focusing on micelles in weakly segregated systems, and to investigate how the mechanisms and time scales involved in micelle formation might affect the final nonequilibrium structures found experimentally in strongly segregated systems. In particular, we investigate how nonequilibrium effects alter the effective scaling of the core radius with Z_{CB}, for example if they cause it to strengthen or to weaken.

The calculation of a suite of autocorrelation times and the system relaxation times forms an integral part of our MC simulations. They are used to indicate the simulation time required to reach equilibrium and, as discussed below, to probe the conditions under which the micelles form and when the polymers begin to be "frozen" in the micelles.

2. Mean Field Study

2.1. Theory. The model used here is a simple model in which all micelles are assumed to be the same size, but it has correctly predicted the behavior of the core radius for micelles consisting of polymers of short core-forming blocks even when experiments have predicted polydisperse sizes.[31] The simple structure of each micelle used in the mean field theory is shown in Figure 1. The total system is separated into three regions. Region 1 contains the cores of micelles, which are composed of the incompatible block of the copolymer plus some solvent. Region 2 is the coronas, consisting of the compatible block and solvent. Region 3 is the solution, which can also contain small amounts of copolymer. The overall volume fractions of copolymer and solvent are denoted by ϕ_C^0 and ϕ_S^0, respectively.

The theory is based on an earlier expression for the free energy.[6,32,34] Since the solvent and both blocks of the copolymer are all different species, we use the expression for the free energy derived by Bluhm and

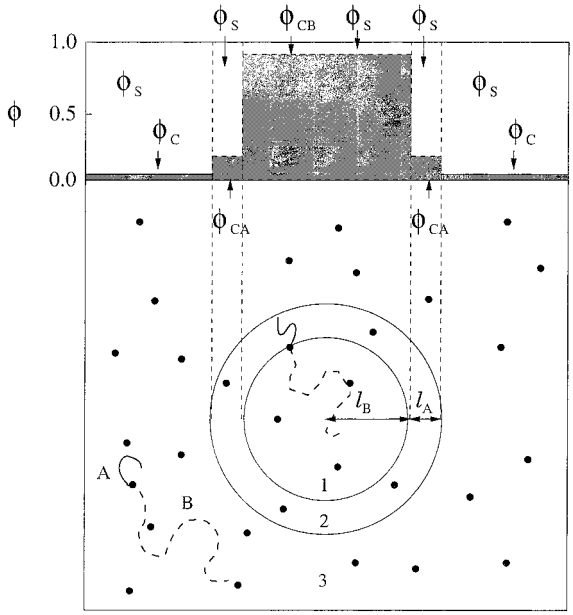

Figure 1. Structure of the crew-cut micelles. Region 1 is the core of the micelle and contains the B block and some solvent. Region 2 is the corona, with A block and solvent. Region 3 is comprised mainly of solvent, with small amounts of copolymer in solution.

Whitmore,[32] with slight modifications. The free energy is approximated by the sum of six terms. These contributions are an enthalpic contribution, two terms from the entropy of mixing of the solvent and the localization of the copolymer joints at the core−corona interfaces, a contribution from the stretching of each polymer block in micelles, one due to the translational entropy of the micelles, and one from the interfacial tension arising from the core−corona interface.

The contribution to the free energy density from the interfacial tension is given by[6,32]

$$g_I = \frac{\gamma}{\rho_0 k_B T}\frac{3l_B^2}{R^3} \qquad (2)$$

where R is the unit cell radius and γ is the interfacial tension. Hong and Noolandi[34] derived an expression from self-consistent field theory for the interfacial tension for a homopolymer-homopolymer interface in the presence of solvent, which was then approximated[5] and used for the interfacial tension at the core−corona interface. When we used this expression for γ, we found that the calculated interfacial width was very small. In particular, it was smaller than the thickness of the depletion layer for polymers end-grafted to a repulsive surface. Because of the presence of a depletion layer, the surface of the core is actually in contact with a layer which is predominantly solvent with a very small concentration of A polymer. A consistent, albeit still approximate, way of calculating γ is to model the interface as an interface between two regions, using the volume fractions in regions 1 and 3.

The free energy depends on four independent parameters, and the equilibrium properties are usually calculated by minimizing the free energy with respect to them. For the strongly segregated systems in this paper, however, we had to impose the additional condition that the solvent chemical potential is equal in regions 1 and 3, i.e., $\mu_S^{(1)} = \mu_S^{(3)}$, in order to eliminate numerical problems. To do this, we use the usual mean field expression[34]

$$\mu_S^{(i)} = \mu_{0S} + 1 - \phi_S^{(i)} + \ln(\phi_S^{(i)}) - \frac{1}{2}\sum_{j,j'}\chi_{j,j'}\phi_j^{(i)}\phi_{j'}^{(i)} \qquad (3)$$

where μ_{0S} is the chemical potential of pure solvent and $\phi_j^{(i)}$ is the volume fraction of component j in region i. This condition reduces the number of independent parameters to three. [In principle, the chemical potential of the solvent should be equal everywhere. However, imposing this condition for all three regions is incompatible with other approximations inherent in this model.]

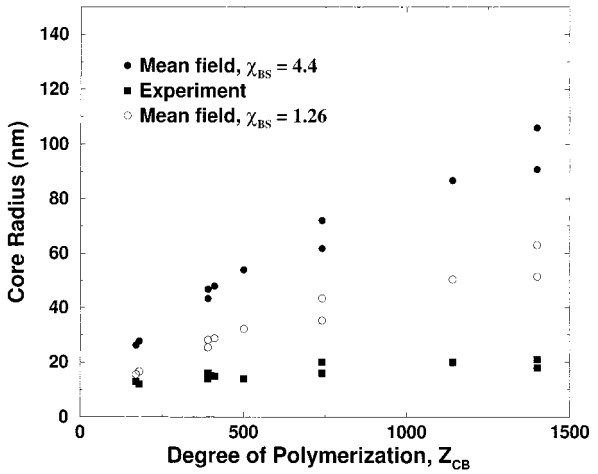

Figure 2. Micelle core radii as functions of the degree of polymerization of the B block, Z_{CB}. The experiments are measurements on dried micelles as described in the text. The theoretical results for $\chi_{BS} = 1.26$ are also adjusted for drying. For $\chi_{BS} = 4.4$, the theory predicts that the micelle cores contain virtually no water before drying, so this adjustment would have no effect.

2.2. Results. Our interest here is in probing the degree to which equilibrium, mean field theory can explain the experimental results of Zhang et al.[1] on crew-cut micelles in water. To do so, we use the most realistic system parameters that are available. For the statistical segment lengths for the A and B blocks, we use[35] $b_A = 0.56$ nm and $b_B = 0.71$ nm, respectively. For the pure component densities, we use $\rho_{0A} = 8.749$ nm^{-3} and $\rho_{0B} = 6.204$ nm^{-3} for the A[35] and B[32] blocks, and $\rho_{0S} = 33.44$ nm^{-3} for the solvent. We did not find accurate values for the Flory interaction parameters in the literature so we estimated them. The solvent is good for the A block, so we chose $\chi_{AS} = 0.2$. Similarly, we set $\chi_{AB} = 0.2$. We found that the results in the strong segregation limit were relatively insensitive to changes in χ_{AS} and χ_{AB} compared to the dependence on χ_{BS}, and our general conclusions are independent of this choice. For PS in water, $\chi_{BS} = 4.4$ for a temperature of 263 °C.[35] As the solvent quality worsens, i.e., lower temperature, χ_{BS} increases. The effect of this is to increase the size of the micelles. As will become clear, our estimates for these parameters are adequate for our purposes.

The experimental and theoretical values of the core radii are plotted as functions of Z_{CB} in Figure 2. In all cases, for $\chi_{BS} = 4.4$, the theoretical cores are much larger than the corresponding experimental ones. In strongly segregated systems such as is the case here, it is believed that the size of the core is determined mainly

by the interplay between the stretching of the B block in the core of the micelle and the interfacial tension.[6] In these experiments the cores are too small for the B block to be significantly stretched. There must, therefore, be a different mechanism that stabilizes the size of the micelles.

The explanation probably lies in the process of micellization. In the experiments, some micelles were prepared using a second method. Both methods involved initially dissolving the polymer in DMF, and then gradually worsening the solvent quality by the addition of water. The second method included an additional step which consisted of adding methanol to the solution of copolymers and DMF before water was added to ensure a gradual change in the solvent property when the water was added. The second method resulted in much larger micelles. This can be explained by the idea that micelles form relatively suddenly as the solvent quality worsens, and they remain trapped in a nonequilibrium state as the solvent quality is further worsened.

In light of this we performed a second mean field calculation intended to simulate conditions of weaker segregation at which micelles might form. For these calculations, the Flory interaction parameter, χ_{BS}, was chosen such that $\phi_{CB} \simeq 0.8$ in the core. This volume fraction is determined by the condition that solvent chemical potentials in regions 1 and 3 are equal. Since the solvent chemical potential in eq 3 does not depend on the degrees of polymerization Z_{CB} and Z_{CA}, this results in the same values of χ_{BS} for all systems, which is $\chi_{BS} = 1.26$.

We also included the effect of drying the micelles. In the experiments, the samples were transferred to copper EM grids, and the water was then evaporated, resulting in decreased core radii. We calculated the radii of dried micelles from the mean field results by

$$R_{core} = \left(\frac{3N_M Z_{CB}}{4\pi\rho_{0B}}\right)^{1/3} \tag{4}$$

where N_M is the number of copolymers per micelle. Henceforth, l_B and R_{core} refer to the radii of the micelle core with and without solvent.

The results are also shown in Figure 2. For all systems, the results are closer to the experimental data compared to the results with $\chi_{BS} = 4.4$, and they are very close for low Z_{CB}. However, for higher degree of polymerization, the predicted core radii are still much larger than in the experiments, by as much as a factor of 3. The core radii and corona thicknesses are well described by power laws of the form of eq 1, with $\alpha = 0.77$ and $\beta = -0.18$, and $l_A \propto Z_{CB}^{\mu} Z_{CA}^{\nu}$ with $\mu = -0.05$ and $\nu = 0.86$, for $\chi_{BS} = 1.26$. The removal of the solvent reduces all radii proportionately, and this would have occurred for any choice of χ_{BS}. Hence, the lack of solvent in the core cannot account for the discrepancy in the scaling results between experiment and theory.

The important conclusion of this section is that, even if we adjust the interaction parameter to mimic micelle formation at relatively weak segregation and allow for the drying of the micelles, equilibrium theory predicts power law scaling for the core radii with a power of about $^2/_3$ or more for these crew-cut micelles and so does not explain the weak power law observed in the experiments.

3. Monte Carlo Study

3.1. Monte Carlo Simulations. The simulations are performed on a cubic lattice of volume $V = L \times L \times L$, where L is the linear dimension of the system. The system contains N_C copolymers, each with Z_C effective monomers, and solvent. Each effective monomer occupies a lattice site, and each empty site corresponds to a solvent molecule. The system is chosen to be large enough to accommodate all the polymers, with the condition that finite size effects are negligible; in all cases L is at least as large as Z_C. Periodic boundary conditions are applied in all directions.

The monomers are subject to excluded volume interactions, so that no more than one monomer can occupy a site. In general, nearest neighbor units interact with an interaction energy E_{ij} (i, j = A, B, S). It is convenient to work with energy parameters given in units of k_BT, i.e. $\epsilon_{ij} = E_{ij}/k_BT$, where k_B is Boltzmann's constant and T the temperature. In the simulations in this paper, the solvent is the same species as the A block of the copolymer, and all interaction energies between like species are set to zero. Therefore, the only nonzero interaction energies are $\epsilon_{AB} = \epsilon_{BS} \equiv \epsilon$.

Except in the test case described below, all simulations reported in this paper use four types of moves to generate new configurations:[36−39] reptation (50%), kink−jump (40%), crankshaft (8%), and Brownian motion (2%). In Brownian motion, the polymer is translated a finite distance without change in shape or orientation. If new sites are occupied, the move is rejected. If the sites are unoccupied, the change in energy is calculated. The probability p of the transition occurring is given by

$$p = \begin{cases} e^{-\beta\Delta E}, & \Delta E > 0 \\ 1, & \Delta E \le 0 \end{cases} \tag{5}$$

where ΔE is the change in energy, and $\beta = 1/k_BT$. A random number r is chosen such that $0 \le r < 1$. The move is accepted if $r \le p$; otherwise, it is rejected. Monte Carlo steps are repeated until equilibrium is reached, and then ensemble averages are taken.

To determine the relevant time scales of the system, various autocorrelation functions and times are calculated. The relaxation time of the system is taken as the maximum of these times.

The first group of autocorrelation functions is defined by

$$C_X(t) = \frac{\langle \vec{X}(t)\cdot\vec{X}(0)\rangle - \langle \vec{X}(t)\rangle\cdot\langle \vec{X}(0)\rangle}{\langle \vec{X}(0)^2\rangle - \langle \vec{X}(0)\rangle^2} \tag{6}$$

where $\vec{X}$ corresponds to the end-to-end vectors of the copolymer and its A and B blocks, $\vec{R}_C$, $\vec{R}_{CA}$ and $\vec{R}_{CB}$, respectively. The symbol $\langle ... \rangle$ denotes an average over time and polymers. The time is measured in N-bead cycles where one N-bead cycle corresponds to N Monte Carlo attempts, with N being the total number of monomers in the system ($N = N_C Z_C$).

Aggregates form in these systems, and it is important to allow time for the polymers to escape and migrate from one aggregate to another. We define an "aggregate" as having two or more B blocks which are in contact with each other. We classify them by three groups. "Small aggregates" have at least 2 but fewer than 10 polymers, "micelles" have at least 10 polymers but their sizes are on the order of molecular dimensions, and

"large aggregates" are macrostructures with a large number of polymers. Reasons for these choices will become clear in later sections. To monitor relevant time scales associated with the polymers in aggregates, we define chain extraction and chain exchange autocorrelation functions by[17]

$$C_f(t) = \frac{\langle f(t)f(0)\rangle}{\langle f(0)^2\rangle} \tag{7}$$

For the chain extraction autocorrelation function, $f(t) = 1$, if the polymer was originally in an aggregate at time $t = 0$ and has not *escaped* the aggregate at time t, and is zero otherwise. For the exchange autocorrelation function, $f(t) = 1$, if the polymer was originally in an aggregate at time $t = 0$ and has not *migrated to another aggregate* at time t, and is zero otherwise. The polymers can exchange between aggregates via single chain or multiple chain exchange. Multiple chain exchange occurs when the aggregates split to form smaller ones, or different aggregates merge to form larger ones. When one aggregate breaks into two smaller ones, the aggregate whose center of mass is closest to the original one is identified as the original aggregate. The other one is identified as the new aggregate, and all its polymers have exchanged. The converse applies for two aggregates that merge.

We also define weighted chain extraction and exchange autocorrelation functions by

$$C_g(t) = \frac{\langle g(t)g(0)\rangle}{\langle g(0)^2\rangle} \tag{8}$$

which give greater weight to polymers in larger aggregates. For the weighted chain extraction function, if a polymer was originally in an aggregate with N_M polymers at time $t = 0$ and has not escaped at time t, then $g(t) = N_M$; $g(t) = 0$ otherwise. Similarly, for the weighted chain exchange function, $g(t) = N_M$ or $g(t) = 0$.

Each autocorrelation function is monitored, and the autocorrelation times τ_i are evaluated using[40]

$$\tau_i = \frac{\int_0^{t_i} C_i(t)dt}{1 - C_i(t_i)} \tag{9}$$

where t_i is defined such that $C_i(t_i) = 1/e$ (i.e. $t_i \simeq \tau_i$) and $i = X, f, g$.

It is also important to allow time for the polymers to move throughout the system. This motion is monitored by calculating a diffusion constant D_C. It is approximated by

$$D_C = \frac{\langle d_C^2(t)\rangle}{6t} \tag{10}$$

where $\vec{d}_C(t) = \vec{r}_C(t) - \vec{r}_C(0)$ is the displacement at time t of the center of mass of the copolymer from its initial position. The time at which the diffusion constant is evaluated corresponds to approximately twice the maximum relaxation time defined by eq 9 for all the quantities defined previously. A relevant time scale is the time required for a free polymer to travel the average distance between nearest neighbor free polymers $\bar{x}$ in the system. It is defined by

$$\tau_{D_C} = \frac{\bar{x}_C^2}{6D_C} \tag{11}$$

with

$$\bar{x}_C \simeq \left(\frac{6V}{\pi N_C}\right)^{1/3} \tag{12}$$

At the beginning of each simulation, the interaction parameter, ϵ, is set to zero and the polymers move randomly for 10 000 N-bead cycles to develop a random configuration. The interaction energy is then increased in small increments. An increase in ϵ corresponds to a decrease in the temperature or an increase in the solvent selectivity. Qualitatively, the latter corresponds to an increase in the water concentration in the experiments of Zhang et al. The system is allowed to equilibrate for a period of 100 relaxation times, and ensemble averages are taken over a period of 200 relaxation times at each value of ϵ. The value of ϵ is then incremented, and the process is repeated.

As the interaction energy is progressively increased, small aggregates begin to form, and at higher ϵ, micellization occurs. Once micelles have formed, the polymer density in the cores is generally high and the enthalpic penalty in removing a polymer from the micelles is large. The result is a large system relaxation time. The simulations are therefore done by slowly increasing ϵ until the required value of ϵ is reached or the computer time required to perform the simulations is excessive. This method allows us to investigate the behavior of the system as a function of solvent quality and pinpoint the highest value of ϵ at which the simulations are feasible. In practice, the simulations are restricted to relatively short polymers and/or small interaction parameter, ϵ.

All simulations were done as single-processor jobs, many on workstations. A typical time required for the simulation of a given system, up to and including micelle formation, is one to two months on a 500 MHz α processor. Numerous simulations are required to calculate scaling relations.

3.2. MC Simulations of a Typical System. We first discuss the micelle characteristics and the behavior of a typical system. It has 1000 copolymers with $Z_{CB} = 50$ and $Z_{CA} = 10$ and an overall volume fraction $\phi_C^0 = 0.02$.

Parts a and b of Figure 3 show the fractions of polymers in small aggregates and micelles, the autocorrelation times, and the time associated with the diffusion of the copolymers, as functions of the interaction parameter, ϵ. As shown in Figure 3a, for $\epsilon \lesssim 0.21$, the fraction of polymers in small aggregates increases slowly with ϵ, while the fraction in micelles remains essentially zero. Beyond $\epsilon \simeq 0.23$, the fraction of polymers in micelles increases sharply while the fraction in small aggregates decreases sharply. These changes are accompanied by an increase in the average size of the micelles. At the largest value of ϵ, 0.248, very few polymers are in small aggregates, although $10.5 \pm 1\%$ of the polymers remain in solution.

Figure 3b shows autocorrelation times for this system. At small ϵ, they are all relatively small and approximately constant. The system contains small, short-lived aggregates with as few as two polymers in each one. There is little or no penalty associated with chain extraction, and the weighted chain extraction time is very short. However, the weighted chain exchange time

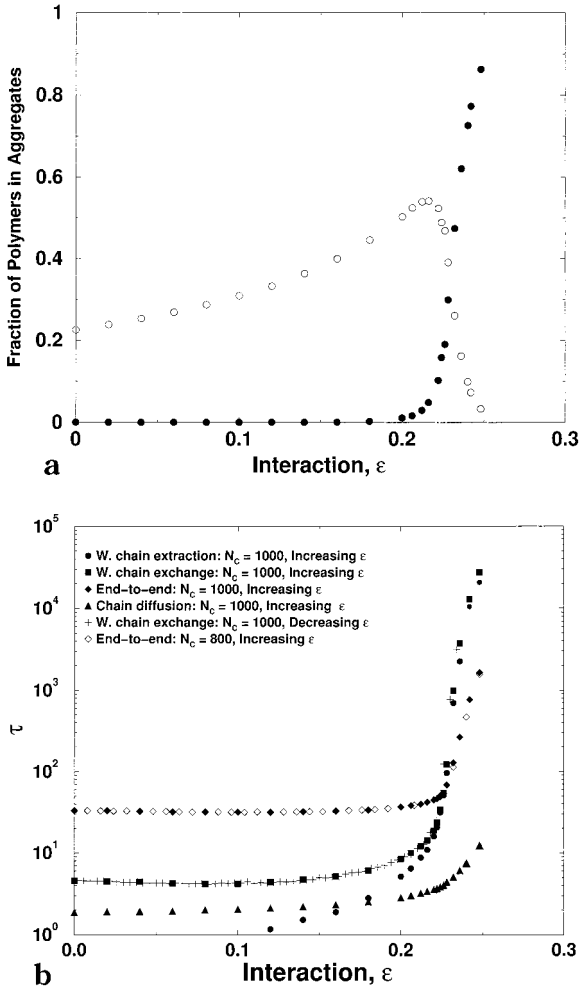

Figure 3. (a) Fraction of polymers in micelles (●) and small aggregates (○) vs ϵ, for $Z_{CB} = 50$, $Z_{CA} = 10$, $\phi_C^0 = 0.02$, and $N_C = 1000$. (b) Semilog plot of the relevant autocorrelation times (in N-bead cycles) as functions of the interaction energy, for $Z_{CB} = 50$, $Z_{CA} = 10$, $\phi_C^0 = 0.02$, and $N_C = 1000$: copolymer extraction (●), copolymer exchange (■), copolymer end-to-end (◆), copolymer diffusion (▲), copolymer exchange with decreasing ϵ (□), and copolymer end-to-end (◇) with $N_C = 800$.

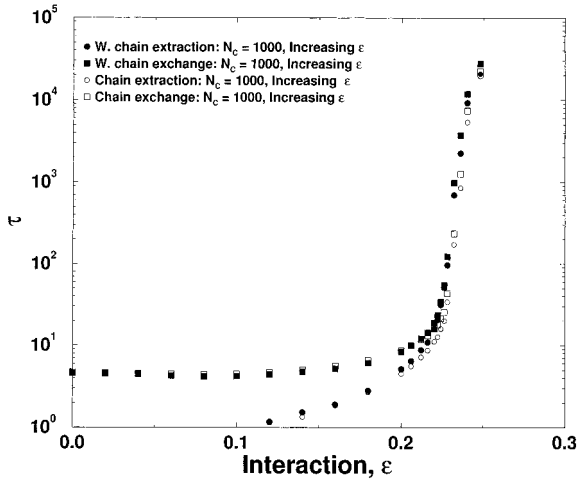

Figure 4. Weighted and nonweighted chain extraction and exchange autocorrelation times (in N-bead cycles) vs ϵ, for $Z_{CB} = 50$, $Z_{CA} = 10$, $\phi_C^0 = 0.02$, and $N_C = 1000$.

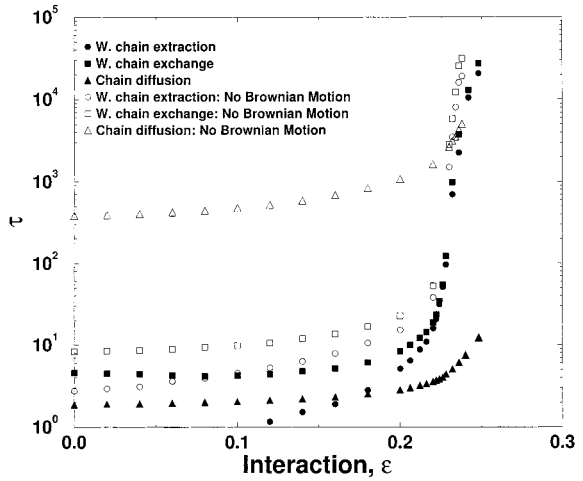

Figure 5. Autocorrelation and diffusion times (in N-bead cycles) with and without Brownian motion, for $Z_{CB} = 50$, $Z_{CA} = 10$, $\phi_C^0 = 0.02$, and $N_C = 1000$.

is much longer. This is because, as shown in Figure 3a, only a small fraction of polymers is in aggregates which results in few aggregates, and in addition, the volume fraction of free chains in solution is small ($\phi_C \simeq 0.017$). Hence, a relatively long time is required for a polymer to come in contact with another polymer or aggregate.

As ϵ increases, the relaxation times begin to increase; when $\epsilon \simeq 0.23$, the weighted extraction and exchange times suddenly increase by nearly 3 orders of magnitude over a small range of ϵ. The copolymer end-to-end vector autocorrelation time and the time associated with the diffusion of polymers, which are quantities averaged over *all* polymers in the system, also increase with decreasing solvent quality. However, the increase in the end-to-end correlation time is modest compared to the weighted extraction and exchange times. The change in the autocorrelation times is consistent with the rapid increase in the fraction of polymers in micelles for $\epsilon \gtrsim 0.23$, as shown in Figure 3a.

Figure 4 compares the chain extraction and *weighted* chain extraction times and the exchange and *weighted* exchange times. When $\epsilon > 0.2$, the weighted extraction time begins to deviate considerably from the extraction time. Differences between the two exchange times are qualitatively similar. We can see from Figure 3a that these differences coincide with a sharp increase in the fraction of polymers in micelles. When the polymers are approximately equally distributed between micelles and small aggregates ($\epsilon \simeq 0.23$), the relative differences between the two extraction and the two exchange times are a maximum. The differences then decrease with increasing ϵ as the fraction of polymers in micelles reaches unity. Nonetheless, when $\epsilon \gtrsim 0.21$ the weighted times are always greater than their nonweighted counterparts. The polymers therefore have long residence times in the micelles compared to their residence times in small aggregates.

Figures 3b and 5 illustrate a few of the tests of our procedures. Figure 3b includes the weighted chain exchange autocorrelation times, calculated first by increasing ϵ from zero to its maximum value and then by decreasing it. The values are the same, independent of the process. Another simulation, with $N_C = 800$, shows a test for finite size effects. Again as shown in Figure 3b, the end-to-end vector autocorrelation times from both simulations agree.

The test shown in Figure 5 is more subtle. All simulations except some of the ones shown in this figure include the mixture of motions identified above, includ-

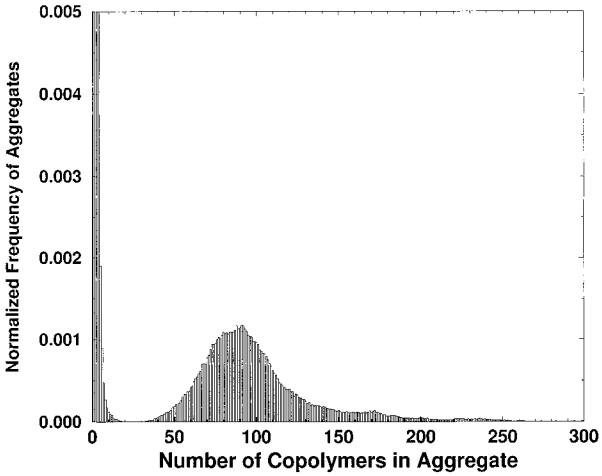

Figure 6. Normalized frequency distribution of aggregates as a function of the number of copolymers in the aggregates, for $\epsilon = 0.248$, $Z_{CB} = 50$, $Z_{CA} = 10$, $\phi_C^0 = 0.02$, and $N_C = 1000$.

ing 2% Brownian motion. These nonlocal moves are useful for speeding up the simulations. However, they can clearly have an effect on any relationship between "simulation" time and "real" time and, perhaps, our association of the sudden increase in the relaxation time with micelle formation. Figure 5 compares results with and without Brownian motion; for the simulations without Brownian motion, the fraction of crankshaft moves was increased from 8% to 10%. Although not shown, the end-to-end correlation times are virtually unchanged over all values of ϵ. At small values of ϵ, the biggest differences are in the diffusion times, with an increase of about 2 orders of magnitude. This is not surprising; there is virtually no energy penalty associated with any move and the polymer concentration is low, so a high proportion of Brownian motion attempts is successful, and they are very effective in moving the molecules through the system. For the same reasons, there are similar, although smaller, effects on the extraction and exchange times. In both sets of simulations, the times increase as ϵ increases and micelles form. The most interesting points are that the sudden increase in relaxation time occurs at almost the same value of ϵ, and that the chain exchange time is the longest one when micelles have formed. The qualitative behavior is unchanged by the inclusion or neglect of Brownian moves, and the quantitative results are modestly changed when micelles are present.

We now turn to the micelle characteristics of this same system, chosen at $\epsilon = 0.248$. Most theoretical approaches assume only a single size for the micelles. Figure 6 displays the frequency distribution of aggregates as a function of the number of polymers in them. There are "small aggregates" with aggregation number up to about 10 and "micelles" with about 40 or more molecules. There is also a rather long tail in the distribution, which is due to micelles whose cores are in contact and are counted as a single large aggregate. Micelles coming in contact with each other can also be observed in visualizations of these systems. These contacts, and the long tails, occur in our simulations only in cases of relatively short corona blocks and low overall degree of polymerization. The relatively thin coronas permit more frequent contact between cores.

To quantify the size distribution of micelles, we calculate the polydispersity index

$$\frac{\bar{N}_w}{\bar{N}_n} = \frac{(\sum_{N=10}^{N_C} M_N N^2)(\sum_{N=10}^{N_C} M_N)}{(\sum_{N=10}^{N_C} M_N N)^2} \quad (13)$$

This summation is over micelles and large aggregates with 10 or more polymers, N is the number of copolymers in a micelle and M_N is the average number of micelles with N polymers. For the distribution in Figure 6, the polydispersity index is 1.14. This calculation includes large aggregates consisting of two or more micelles. To approximately correct for this, we also performed a Gaussian fit to the distribution of micelles with N ranging from 30 to 120 and calculated the polydispersity index from it. The resulting value was 1.05. The long tail therefore significantly contributes to the polydispersity. These values compare with the experimental value of 1.08 for crew-cut micelles observed by Zhang et. al.[1]

Figure 7a shows the polymer volume fraction profiles, averaged over micelles with 86 to 100 copolymers, at $\epsilon = 0.248$. [Each aggregate was collected into one of 10 bins with each bin having the same interval spacing except for the first and last bins. The first bin identifies aggregates with 10 or fewer polymers while the last bin identifies the larger aggregates. The resulting interval width is 15, and the bin corresponding to the range 86−100 polymers is chosen for these volume fraction profiles because it contains the maximum in the distribution of micelles, shown in Figure 6.] In general, averaging over all micelles tends to broaden the interface, and the size specific averaging is therefore done to better characterize the volume fraction profiles. In the core of these micelles, the polymer volume fraction is as high as 0.82. The results that the maximum volume fraction of the copolymer in the core is well below unity, and approximately 10% of the polymers remain in solution, indicate that the system is weakly segregated. As noted earlier, most experiments are in the limit of strong segregation. Nonetheless, it is interesting to compare information about the structure of the micelles and other characteristics of the system. As assumed in the mean field model, the volume fraction profile in the core is essentially uniform. However, the profile of the A block in the corona, $\phi_{CA}(r)$, is not, as was suggested by Halperin,[8] and is more like the profiles observed in previous SCF[13] and SCMF[14] calculations. What is most striking in Figure 7a is the poorly defined core−corona interface: In fact, the corona itself is not even well-defined, with $\phi_{CB}(r) \gtrsim \phi_{CA}(r)$ throughout most of it. We attribute this to the facts that the corona block is short and the system is weakly segregated.

The similarity of the scaling results of Halperin's model with those of other models with constant density profiles (see Table 1) implies that the approximation of uniform profiles does not affect the scaling relations significantly. Therefore, the fact that $\phi_{CA}(r)$ is not constant should not account for the discrepancy with the recent experimental results.

Figure 7b and its inset display normalized distributions and volume fractions, respectively, of the free A and B ends and the A−B joints of the copolymer. In principle, the distributions could be calculated directly from the number of ends or joints present in each shell of radius r about the center of mass of the micelle. To a

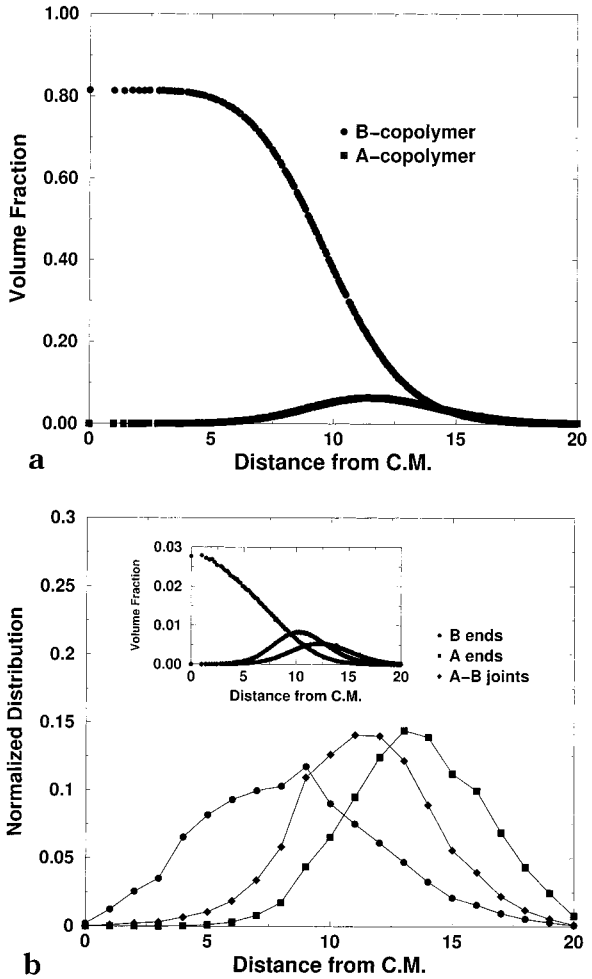

Figure 7. (a) Volume fraction profiles of A and B blocks as functions of the distance from the center of mass (C.M.) of the micelles, for $\epsilon = 0.248$, $Z_{CB} = 50$, $Z_{CA} = 10$, $\phi_C^0 = 0.02$, and $N_C = 1000$. (b) Normalized distributions of A and B ends and A−B joints as functions of the distance from the center of mass (C.M.) of the micelles, for $\epsilon = 0.248$, $Z_{CB} = 50$, $Z_{CA} = 10$, $\phi_C^0 = 0.02$, and $N_C = 1000$. The inset shows the volume fraction profiles of A and B ends and A−B joints. The lines are shown as a guide to the eye only.

first approximation, the distribution of sites varies as Ar^2 where A is a constant, but the underlying lattice introduces large fluctuations. To reduce the effects of these variations, the data are collected in bins of unit width. A single bin can include several shells, and this results in a somewhat smoother distribution of available sites.

The A and B ends and A−B joints are all broadly distributed. All distributions decrease nearly to zero at the center of mass of the micelle, since the number of sites decreases to unity. However, the volume fraction of B ends is a maximum at $r = 0$, as shown in the inset. This means that the B ends penetrate to the center of the micelle core as assumed in the mean field picture, but they are distributed throughout the core. This result is consistent with previous MC simulations[19] and experiments.[41] For the A ends, the peak in the distribution is shifted slightly to the outer portion of the corona relative to the peak in $\phi_{CA}(r)$ shown in Figure 7a. The distribution of joints shows a maximum at the interface, and the broad distribution is consistent with a poorly defined interface.

The volume fraction of the B ends shown in the inset of Figure 7b decreases more rapidly with increasing r than the volume fraction of the B block, $\phi_{CB}(r)$, shown in Figure 7a. This provides further evidence that the B ends tend to reside in the center of the core compared to the rest of the B block. The peak in the volume fraction of A ends in the inset is shifted slightly to a higher value of r compared to the peak in $\phi_{CA}(r)$ shown in Figure 7a. This indicates that the A copolymer ends tend to reside toward the outer edges of the corona. Nonetheless, the distribution of A ends shows that a considerable fraction of them is distributed throughout the corona.

Table 2. Results for the Radius of Aggregate Cores (R_{core}), the Number of Copolymers Per Aggregate (N_M), and the Reduced Interaction Energy (ϵ_c) for $\tau_c = 8000$ and $\tau_c = 12\,000$ from MC Simulations at Different Molecular Weights

system			$\tau_c = 8000$			$\tau_c = 12\,000$		
Z_{CB}	Z_{CA}	N_C	ϵ_c	N_M	R_{core}	ϵ_c	N_M	R_{core}
20	4	1000	0.320	91	7.58	0.325	111	8.09
30	6	1000	0.279	78	8.23	0.283	88	8.59
40	8	1000	0.254	68	8.64	0.256	73	8.88
50	10	1000	0.240	64	9.13	0.242	69	9.38
60	12	1000	0.228	54	9.17	0.230	64	9.71
20	10	1000	0.332	40	5.76	0.339	47	6.07

3.3. Scaling Results. In this section, a series of MC simulations is described which are aimed at investigating how nonequilibrium effects can account for the discrepancy between the power laws predicted by existing equilibrium theories and the recent experiments. The basic idea is to use our calculation of relaxation times to identify the value of ϵ for each system at which the micelle structures are effectively "frozen in". We follow our usual procedure of slowly increasing ϵ but, instead of comparing systems at a common ϵ (or χ in the mean field theories), we make the comparisons at a common relaxation time, τ_c, which we choose up in the range where micelles have formed. This corresponds to different values of ϵ, which we label ϵ_c, for each system. We will conclude by calculating the scaling with molecular weight at common τ, thus investigating, approximately, the scaling relation at the solvent quality at which each system becomes frozen in. Of course, comparing these results with experiment is valid only to the extent that simulation time is proportional to real time. This is always an open question, and our comparisons cannot be considered quantitative.

We used two values of τ_c, 8000 and 12 000 N-bead cycles. To some extent, these choices are arbitrary, but micelles have formed in all cases, except for one as discussed below, and our results are qualitatively the same for each choice, which suggests that the particular value chosen does not affect our general conclusions. The radii of the micelle cores, the average numbers of copolymers per micelle, and the reduced interaction energies at which the system relaxation time is τ_c in each case, are shown in Table 2. We calculated the core radii from eq 4 with $\rho_{0B} = 1$ to simulate "dried" micelles.

As shown in Figure 3b, there can be a large change in the system relaxation time for a relatively small increment in ϵ. It is therefore difficult to determine, a priori, the interaction, ϵ_c, for which $\tau = \tau_c$. To determine ϵ_c, we performed an interpolation of the weighted chain exchange autocorrelation time as a function of ϵ. From our interpolation we determined the values of ϵ at which the weighted chain exchange autocorrelation time is equal to τ_c. At each value of ϵ we performed a Gaussian fit to the distribution of micelles as a function of the

number of copolymers per micelle. The average number of polymers in micelles, N_M, was determined from the maximum of the Gaussian fits. An interpolation of N_M as a function of ϵ was also performed to determine N_M at ϵ_c. This method of determining the average number of polymers per micelle is adequate since the relative change in N_M is small compared to the change in τ with increasing ϵ. Uncertainties in N_M due to the interpolation are only a few percent.

The system with $Z_{CB} = 20$ and $Z_{CA} = 4$ behaves differently than the rest. When the system relaxation time exceeds about 10 000 N-bead cycles, very large nonspherical aggregates begin to form, showing signs of macrophase separation. To examine the effect of the corona block, we also performed simulations for $Z_{CB} = 20$ and $Z_{CA} = 10$. The results are included in Table 2. In this case there is a narrow distribution of micelles with no large aggregates. Our simulations with constant Z_{CA}/Z_{CB} also show that the width of the size distribution of micelles decreases with increasing Z_C. Nonetheless, as shown earlier from the simulation with $Z_{CB} = 50$ and $Z_{CA} = 10$, even when $Z_C = 60$ there remains a long tail in the distribution of micelles. The presence of large aggregates in the simulation with $Z_{CB} = 20$ and $Z_{CA} = 4$ is therefore attributed to the relatively short corona block compared to the core block, augmented by the fact that Z_C is small.

The reduced interaction energy at which the copolymers begin to be trapped in the aggregates decreases with increasing molecular weight of the copolymer, as expected from the mean field predictions. Figure 8a shows a plot of the product $\epsilon_c Z_{CB}$ as a function of the chain length Z_{CB} for both $\tau_c = 8000$ and $\tau_c = 12\,000$. The plot shows a linear increase with Z_{CB} which can be expressed as

$$\epsilon_c Z_{CB} = m Z_{CB} + b \tag{14}$$

with $m = 0.177 \pm 0.003$ and $b = 3.09 \pm 0.13$ for $\tau_c = 8000$ and $m = 0.178 \pm 0.002$ and $b = 3.17 \pm 0.08$ for $\tau_c = 12\,000$.

In Figure 8b, the core radii of the dried micelles are plotted on a log−log graph as a function of Z_{CB} for both choices of τ_c. Although N_M decreases with increasing molecular weight of the copolymer, as seen in Table 2, the core radii increase. The curves imply $R_{core} \propto Z_{CB}^{\alpha}$ with $\alpha = 0.18 \pm 0.02$ for $\tau_c = 8000$ and $\alpha = 0.17 \pm 0.03$ for $\tau_c = 12\,000$; the value of α is essentially independent of our choices of τ_c. It is lower than the experimental value of about 0.4, and much less than the equilibrium mean field values of about $^2/_3$.

The important point of this section is that these MC simulations indicate that the use of a constant system relaxation time as a criterion for the solvent quality at which the micelle characteristics are calculated can explain a weaker power law, as observed experimentally, and the change can be quite large. We reemphasize, however, that quantitative results would depend on knowing the relationship between simulation and real times and, perhaps, on knowing the best value of τ_C.

4. Summary

We have performed simple mean field calculations and Monte Carlo simulations of block copolymer micelles. The mean field calculations were used to explore equilibrium scaling relations for crew-cut micelles, and if recent experiments could be understood within the context of equilibrium, mean field theory. The MC simulations were used to probe the micelle structure and the distribution of micelle sizes and to determine whether the weak dependence of the core radii on the degree of polymerization of the core-forming block of the copolymer, as observed by Zhang et al.,[1] can be understood on the basis of relaxation times.

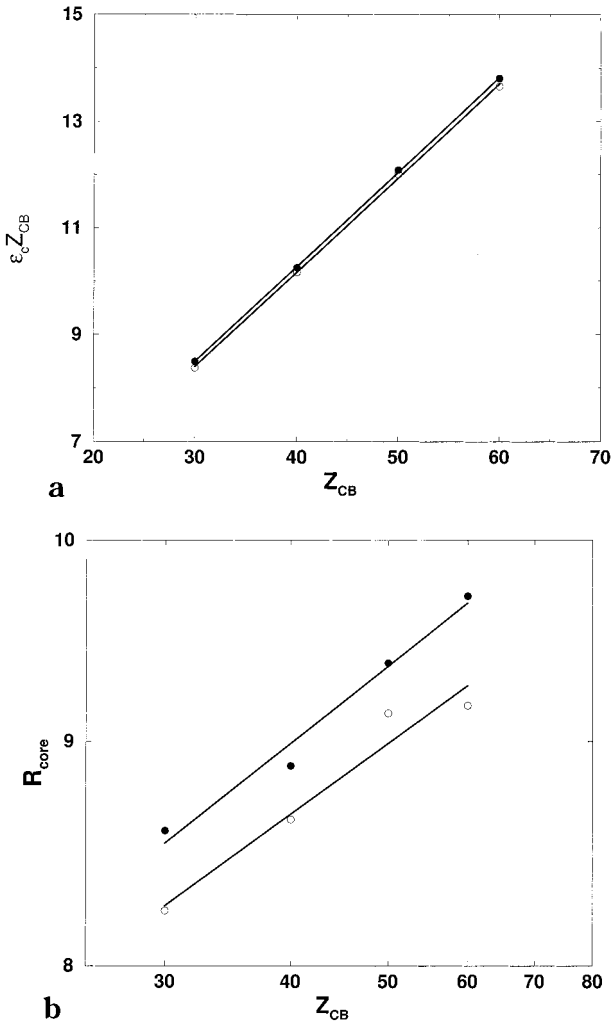

Figure 8. (a) Product of the reduced interaction energy and the chain length of the B block vs the chain length of the B block. The open and closed symbols correspond to $\tau_c = 8000$ and $\tau_c = 12\,000$, respectively. The straight lines correspond to the lines of best fit. (b) Radius of the micelle core, R_{core}, as a function of chain length of the B block, at constant τ_c. The open and closed symbols correspond to $\tau_c = 8000$ and $\tau_c = 12\,000$, respectively. The straight lines correspond to the lines of best fit.

The mean field theory predicts micelles with core radii and aggregation numbers much larger than those found in the experiments, and stronger power law dependences that are comparable with those usually found for micelles. In fact, the calculations imply that the observed micelles are too small to have significantly stretched core blocks, which is in strong contrast with what one would expect for very strongly segregated systems. We also explored the possibility that the observations could be explained by micelle formation at a lower segregation regime, but were unable to reproduce weaker power law dependences within this equilibrium theory.

The critical micelle concentration and the energy barrier associated with a polymer escaping from one

micelle and moving to another depend on both the polymer molecular weight and the solvent quality. This implies that the solvent quality at which a micelle system "freezes" depends on the molecular weight. This was one of the motivations for our MC simulations, in which we explicitly calculate system relaxation times, although the connection between Monte Carlo time and real time is unclear.

In all cases, the system relaxation time increases with interaction energy, and the increase becomes dramatic as micelles form. When we calculated the micelle characteristics for different systems at a common value of the relaxation time, rather than a common solvent quality or interaction energy, we obtained a much weaker power law dependence for the core radii. These results are consistent with the idea that the strong dependence of the relaxation times on the molecular weight of the B block can account for a weaker scaling, as observed.

We also used the MC simulations to explore the micellar structures. The cores are comprised of the B block of the copolymer and solvent, and each one is relatively uniform, as assumed in mean field theory. However, the A block, which normally forms the corona, has a nonuniform density profile. This is inconsistent with the structure of the corona region assumed in many mean field theories, although the work of Halperin[8] suggests that this assumption does not significantly affect the scaling behavior. The distributions of copolymer ends and the A−B copolymer joints were also investigated. The B ends penetrate to the center of the micelles and the A ends extend to the edge of the corona. However, the A and B ends are also present throughout corona and core regions, respectively. The A−B joints are distributed across a relatively broad interface which is not well defined. This is attributed to a low molecular weight corona block and weak segregation. The presence of a significant amount of copolymer in solution, along with a considerable amount of solvent in the cores of the micelles, also indicates that the systems are weakly segregated.

The distribution of micelle sizes was relatively narrow, except for a long tail. The tail is attributed to micelles in contact with each other, which can occur because of the short A block. The calculated polydispersity index for the micelles (excluding the tail) was 1.05, which compares well with the polydispersity of 1.08 observed in experiments.[1]

Acknowledgment. We thank Dr. G. Slater, Sylvain Hubert, and Martin Kenward for contributions to the work, and we acknowledge the computing resources offered through Canada's C3.ca program at Université de Montréal, University of Alberta, Unversity of Calgary, and Memorial University of Newfoundland. This work is funded in part by the Natural Sciences and Engineering Research Council of Canada.

References and Notes

(1) Zhang, L.; Barlow, R. J.; Eisenberg, A. *Macromolecules* **1995**, *28*, 6055.
(2) Gao, Z.; Varshney, S. K.; Wong, S.; Eisenberg, A. *Macromolecules* **1994**, *27*, 7923.
(3) Liebert, J. Ed. *Solid State Physics*; Academic: New York, 1978. Supplement 14.
(4) Leibler, L.; Orland, H.; Wheeler, J. C. *J. Chem. Phys.* **1983**, *79*, 3550.
(5) Noolandi, J.; Hong, K. M. *Macromolecules* **1983**, *16*, 1443.
(6) Whitmore, M. D.; Noolandi, J. *Macromolecules* **1985**, *18*, 657.
(7) Nagarajan, R.; Ganesh, K. *J. Chem. Phys.* **1989**, *90*, 5843.
(8) Halperin, A. *Macromolecules* **1987**, *20*, 2943.
(9) Daoud, M.; Cotton, J. P. *J. Phys. (Les Ulis, Fr.)* **1982**, *43*, 531.
(10) Linse, P. *Macromolecules* **1994**, *27*, 2685.
(11) Leermakers, F. A. M.; Wijmans, C. M.; Fleer, G. J. *Macromolecules* **1995**, *28*, 3434.
(12) Linse, P.; Malmsten, M. *Macromolecules* **1992**, *25*, 5434.
(13) Wijmans, C.; Linse, P. *Langmuir* **1995**, *11*, 3748.
(14) Mackie, A. D.; Panagiotopoulos, A.; Szleifer, I. *Langmuir* **1997**, *13*, 5022.
(15) Guerin, C.; Szleifer, I. *Langmuir* **1999**, *15*, 7901.
(16) Smit, B.; Esselink, K.; Hilbers, P. A. J.; van Os, N. M.; Rupert, L. A. M.; Szleifer, I. *Langmuir* **1993**, *9*, 9.
(17) Haliloğlu, T.; Mattice, W. L. *Polym. Prepr.* **1993**, *34*, 460.
(18) Rodrigues, K.; Mattice, W. L. *Polym. Bull.* **1991**, *25*, 239.
(19) Rodrigues, K.; Mattice, W. L. *J. Chem. Phys.* **1991**, *95*, 5341.
(20) Rodrigues, K.; Mattice, W. L. *Langmuir* **1992**, *8*, 456.
(21) Wang, Y.; Mattice, W. L.; Napper, D. H. *Langmuir* **1993**, *9*, 66.
(22) Zhang, Y.; Mattice, W. L. *Macromolecules* **1994**, *27*, 677.
(23) Zhang, Y.; Mattice, W. L. *Macromolecules* **1994**, *27*, 683.
(24) Rodrigues, K.; Mattice, W. L. *J. Chem. Phys.* **1991**, *94*, 761.
(25) Nguyen-Misra, M.; Mattice, W. L. *Macromolecules* **1995**, *28*, 1444.
(26) Haliloğlu, T.; Bahar, I.; Erman, B.; Mattice, W. L. *Macromolecules* **1996**, *29*, 4764.
(27) Cogan, K. A.; Gast, A. P.; Capel, M. *Macromolecules* **1991**, *24*, 6512.
(28) Selb, J.; Marie, P.; Rameau, A.; Duplessix, R.; Gallot, Y. *Polym. Bull.* **1983**, *10*, 444.
(29) Tao, J.; Stewart, S.; Liu, G.; Yang, M. *Macromolecules* **1997**, *30*, 2738.
(30) Kinning, D. J.; Thomas, E. L.; Fetters, L. J. *J. Chem. Phys.* **1989**, *90*, 5806.
(31) Qin, A.; Tian, M.; Ramireddy, C.; Webber, S. E.; Munk, P.; Tuzar, Z. *Macromolecules* **1994**, *27*, 120.
(32) Bluhm, T. L.; Whitmore, M. D. *Can. J. Chem.* **1985**, *63*, 249.
(33) Hurtrez, G. Etude des Copolymères Séquencés poly(Styrène-*b*-Oxyde d'Ethylene) Synthèse, Propriétés Colloïdales et Tensio-actives, Ph.D. Thesis, Université de Haute Alsace, Mulhouse, France, 1992.
(34) Hong, K. M.; Noolandi, J. *Macromolecules* **1981**, *14*, 727.
(35) Brandup, J.; Immergut, E. H. *Polymer Handbook*, 3rd ed.; John Wiley and Sons Inc.: New York, 1989.
(36) Verdier, P. H.; Stockmayer, W. H. *J. Chem. Phys.* **1962**, *36*, 227.
(37) Domb, C. *Adv. Chem. Phys.* **1962**, *15*, 229.
(38) Hilhorst, H. J.; Deutch, J. M. *J. Chem. Phys.* **1975**, *63*, 5153.
(39) Gurler, M. T.; Crabb, C. C.; Dahlin, D. M.; Kovak, J. *Macromolecules* **1983**, *16*, 398.
(40) Murat, M.; Grest, G. S. *Macromolecules* **1989**, *22*, 4054.
(41) Rodrigues, K.; Kaush, C. M.; Kim, J.; Quirk, R. P.; Mattice, W. L. *Polym. Bull.* **1991**, *26*, 695.

MA992135Z